

Jie Zhu, Xue-Jing Zhao, Peng-Cheng Wang, and Ming Lu*

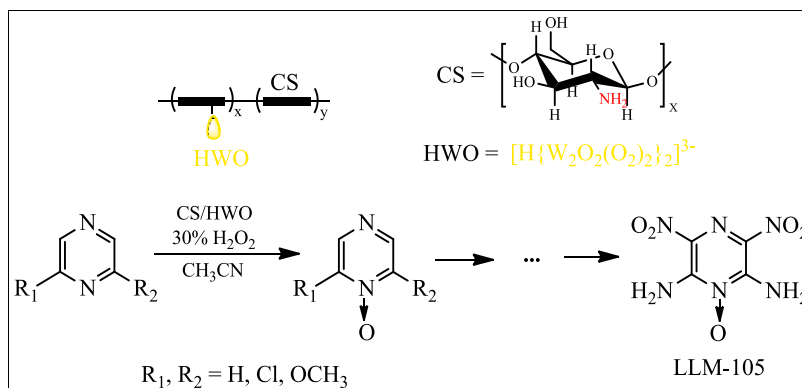
Chemical Engineering College, Nanjing University of Science and Technology, Nanjing 210094, China

*E-mail: luming302@126.com

Received January 29, 2013

DOI 10.1002/jhet.2044

Published online 00 Month 2016 in Wiley Online Library (wileyonlinelibrary.com).



A new catalytic system was developed and applied to the oxidation reactions involved in the synthesis of LLM-105, in which protonated peroxotungstate combining chitosan was used as catalyst. With H₂O₂ as oxidant, good to excellent yields could be achieved in the synthesis of pyrazine-1-oxide, 2,6-dimethoxypyrazine-1-oxide, 2,6-dichloropyrazine-1-oxide, and 2-chloro-6-methoxypyrazine-1-oxide without any addition of trifluoroacetic acid, which provided a significant exploration toward novel and environmentally benign synthetic route for LLM-105. Theoretical studies were also carried out with Gaussian 03 to evaluate the oxidation process. All of the calculated data matched well with our experimental results.

J. Heterocyclic Chem., **00**, 00 (2016).

INTRODUCTION

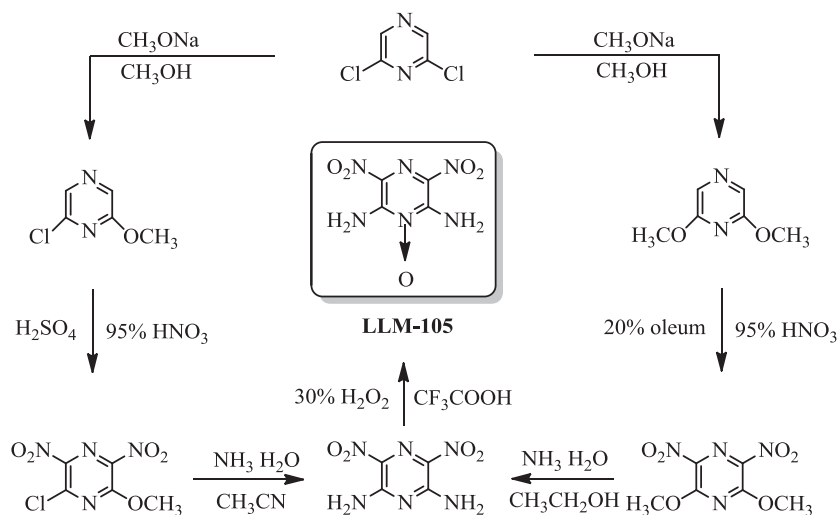
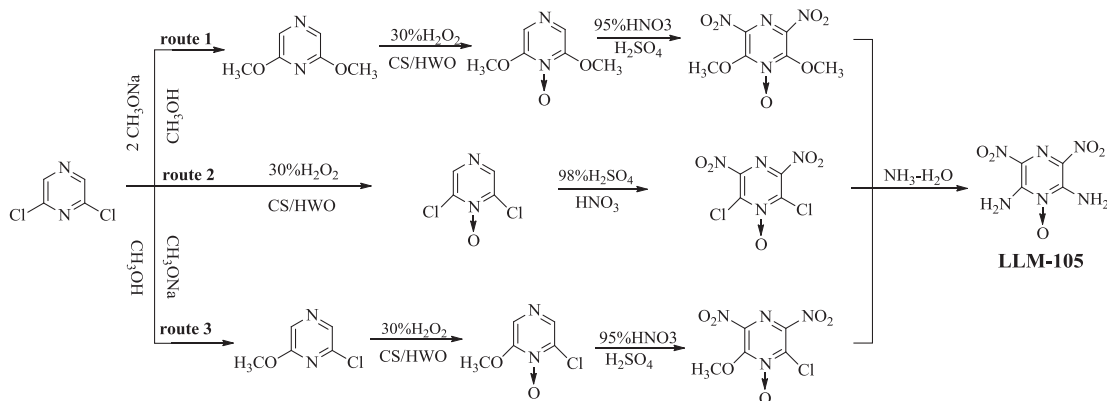
There is a continuing need for developing energetic materials because of their numerous military and industrial applications. The general requirements for these potential materials mainly include: high density and energy, thermal stability/storability and low handling hazards (e.g., low sensitivity to impact, friction, electrostatic discharge, and low toxicity) [1]. Considering the comprehensive properties, 2,6-diamino-3,5-dinitropyrazine-1-oxide (LLM-105) has emerged to show great application prospect because of the existence of hydrogen bond in and between each molecule leading to a crystal density at ambient as high as 1.91 g/cm³. And its energy was 20% higher than that of 2,4,6-triamino-1,3,5-trinitrobenzene (TATB) but showed similar impact sensitivity with TATB [2].

The Lawrence Livermore National Laboratory had got outstanding achievements for energetic materials researches and synthesized LLM-105 completely for the first time in 1995, which was published several years later [3]. After that, P. F. Pagoria improved the synthetic route of LLM-105 as shown in Scheme 1 to achieve higher yields, fewer steps, and shorter reaction period [4]. Then in 2001, on the base of Scheme 1, Tran and Li further modified the synthetic route by using 2,6-dimethoxypyrazine instead of the intermediate 2-chloro-6-methoxypyrazine (1), a highly

volatile liquid at room temperature, which is difficult to dry and preserve [5].

However, Scheme 1 uses of plenty trifluoroacetic acid to proceed with the oxidation reaction, which was expensive, corrosive, and difficult to recover, as well as leading to bothersome post-treatment and serious environmental pollution [6]. If LLM-105 could be produced without the use of trifluoroacetic acid, manufacturing cost would be decreased significantly and easy scale-up would be achieved. In many countries, much attention has been paid on the development of new synthetic route of LLM-105, as well as with the main purpose of avoiding the use of trifluoroacetic acid [7]. For the same goal, we proposed three experimental formulas as shown in Scheme 2 (route 1, 2, and 3), expecting to find a better design route. The synthetic routes went through similar procedures including nitration and ammoniation, and the oxidation process became a pivotal step.

Herein, in this paper, a new catalytic system was developed and applied to the oxidation reactions involved in the synthesis of LLM-105, in which protonated peroxotungstate combining CS was used as catalyst. Good to excellent yields could be achieved with pyrazine, 2,6-dimethoxypyrazine, 2,6-dichloropyrazine, and 2-chloro-6-methoxypyrazine as substrates. Trifluoroacetic acid was avoided completely in the reactions that represent a significant step towards the

Scheme 1. Synthetic route of LLM-105 improved by P. F. Pagoria.**Scheme 2.** Proposed synthetic route for LLM-105 to avoid trifluoroacetic acid.

new synthetic route for LLM-105. And theoretical studies were carried out to explore the influence of functional groups on pyrazine to the oxidation process. The energy and natural bond orbital (NBO) was investigated to describe the nature of the intermediates.

RESULTS AND DISCUSSION

Preparation and characterization of the catalyst. Recently, peroxotungstate has emerged as an effective catalyst for selective oxygen transfer to organic substrates with H_2O_2 as a terminal oxidant [8]. Despite of the high activity, the utilization of H_2O_2 is relatively low because excessive H_2O_2 was needed. To circumvent the problem, Ishimoto developed a protonated peroxotungstate $\text{TPA}_3[\text{H}\{\text{W}_2\text{O}_2(\text{O}_2)_4(\mu-\text{O})\}_2]$ ($\text{TPA} = [(\text{n}-\text{C}_3\text{H}_7)_4\text{N}]^+$), which showed high catalytic activity and increased the utilization rate of H_2O_2 [9]. To introduce the system into the oxidation of pyrazine derivatives, protonated peroxotungstate catalyst

with different cations were prepared and tested because TPAOH, the raw material of $\text{TPA}_3[\text{H}\{\text{W}_2\text{O}_2(\text{O}_2)_4(\mu-\text{O})\}_2]$, is a little expensive for industrial production. Instead, hexadecyl trimethyl ammonium bromide and tetrabutyl ammonium bromide were tried respectively. Catalysts were obtained through filtration after the protonation process. The yields for catalyst preparation with CTA and TBA cations, however, were very low as both hexadecyl trimethyl ammonium bromide/HWO and tetrabutyl ammonium bromide/HWO could dissolve a little in water. Water addition would not facilitate the separation of catalysts, and thus the catalyst isolation remained to be a problem.

Chitosan (CS), a linear polymer of (1-4)-linked 2-amino-2-deoxy-gucopyranose, is generally regarded to be nontoxic, biocompatible, and biodegradable. The free amines in CS provide various opportunities for chemical modification to obtain different CS derivatives [10], which makes CS an excellent candidate to serve as the cation of protonated peroxotungstate.

The IR spectrum (Fig. 1) of CS/HWO (line d) showed detectable peaks that are characteristic of CS (line b) around 1150 and 3460 cm⁻¹. IR bands belong to the W-O vibrations at 803 and 895 cm⁻¹ were also exhibited in CS/HWO [11], which clearly differed from that of H₂WO₄ (line a). Minor differences could be detected as well at these bands when compared with that of CS/WO (line c), suggesting the successful protonation process of CS/WO. These facts are consistent with the synthesis design and confirm the successful combination of CS and protonated peroxotungstate.

Thermogravimetric (TG) studies showing the TG curves for CS/HWO, CS/WO, and pure CS were also carried out to help to characterize the catalyst as shown in Figure 2. Within 200°C, the weight loss was probably attributed completely to the absorbed water molecules. The catalyst CS/HWO went through a similar process of weight loss compared with that of pure CS, whereas the total amount

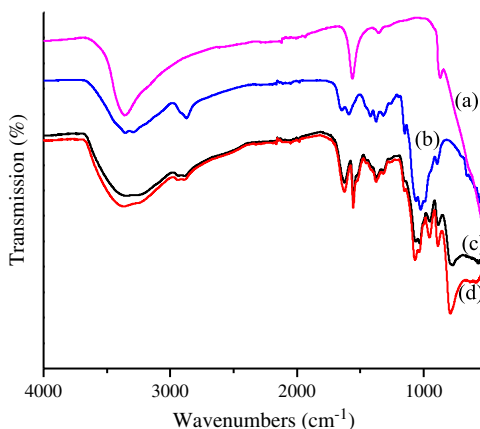


Figure 1. IR spectrum of (a) H₂WO₄; (b) chitosan (CS); (c) CS/WO; and (d) CS/HWO. [Color figure can be viewed in the online issue, which is available at wileyonlinelibrary.com.]

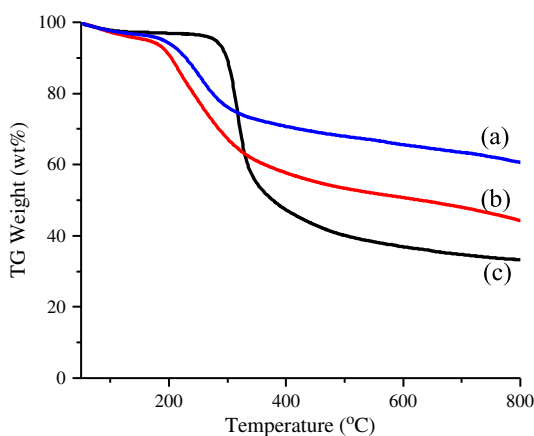


Figure 2. TG curves of (a) CS/HWO; (b) CS/WO, and (c) pure CS. [Color figure can be viewed in the online issue, which is available at wileyonlinelibrary.com.]

of weight loss reduced obviously, which was supposed to be because of the existence of protonated peroxotungstate, indicating the successful combination process. At around 300°C, the TG curve of CS/HWO was not as sharp as that of pure CS and CS/WO with a little advanced weight loss as well. This was probably attributed to the protonation process with the introduction of H to every peroxotungstate, leading to an increased proportion of W along with a decreased weight loss.

The affecting factors in oxidation process. To screen the optimal oxidation conditions, key factors that affecting the oxidation process were fully evaluated with 2,6-dichloropyrazine as model substrate, including the catalytic system, the amount of H₂O₂, the amount of catalyst (Fig. 3), and the temperature.

Catalytic system no doubt had a fundamental influence on the oxidation process. Comparative experiments under different catalytic systems mentioned previously were carried out as listed in Table 1. It was found that almost no product was obtained in acetonitrile only without any catalyst (entry 2) or with CS only without peroxotungstate (entry 3). Oxidation yield remained almost constant when altering the cation of protonated peroxotungstate (entries 4–7). The yield of catalyst preparation, however, differs much with CS/HWO exhibiting the highest preparation yield because of its immiscibility with water. Taken that into consideration, CH₃CN–CS/HWO system showing the highest multiplied yields was chosen for the following oxidation process. Comparable results could be obtained under CF₃COOH–H₂O₂ and CH₃CN–CS/HWO–H₂O₂ systems, suggesting that novel oxidation process for synthesis of LLM-105 intermediates without CF₃COOH was possible to be achieved.

Under the CH₃CN–CS/HWO system, synthesis of 2,6-dichloropyrazine-1-oxide with variant reaction conditions were further conducted, and the results are summarized in Table 2. CS/HWO of catalytic amount was enough to initiate

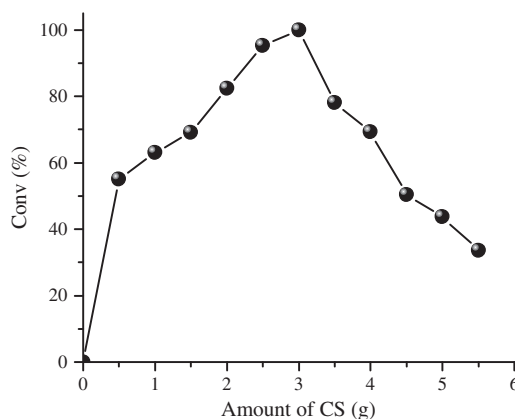
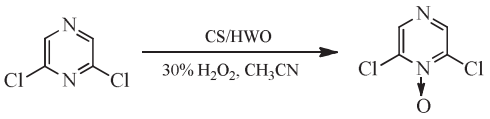
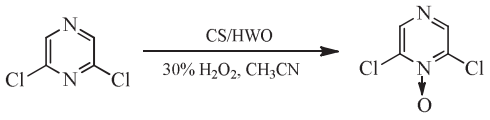


Figure 3. Synthesis of 2,6-dichloropyrazine-1-oxide catalyzed by CS/HWO with different amounts of CS.

Table 1Synthesis of 2,6-dichloropyrazine-1-oxide under different catalytic systems^a.


Entry	Oxidation system	t/h	Yield/%	Multiplied yield/%
1	CF ₃ COOH	2	89	89
2	CH ₃ CN	12	trace	trace
3	CH ₃ CN-CS	12	trace	trace
4	CH₃CN-CS/HWO	4	73	62
5	CH ₃ CN-CTA/HWO	7	70	29
6	CH ₃ CN-TBA/HWO	5	71	33
7	CH ₃ CN-TPA/HWO	4	75	57

^aReaction conditions: 2,6-dichloropyrazine 10 mmol, solvent 30 mL, 30% H₂O₂ 5 mL was added five times equably during the reaction time, 60°C.**Table 2**Synthesis of 2,6-dichloropyrazine-1-oxide with variant reaction conditions^a.


Entry	CS/HWO (mmol)	30% H ₂ O ₂ (mL)	T (°C)	t (h)	Conv (%)	Yield (%)
1	0.05	5	60	6	98	66
2	0.1	5	60	5	100	69
3	0.2	5	60	5	100	69
4	0.1	1	60	8	82	43
5	0.1	3	60	8	96	48
6	0.1	10	60	4	100	70
7	0.1	5^b	60	4	100	73
8	0.1	5 ^b	25	12	51	36
9	0.1	5 ^b	40	8	70	49
10	0.1	8 ^b	80	4	100	72
11	0.1	5 ^b	60	2	83	54
12	0.1	5 ^b	60	8	100	65
13	0.1	5 ^b	60	12	100	58

^aReaction conditions: 2,6-dichloropyrazine 10 mmol, CH₃CN 30 mL.^bH₂O₂ 5 mL was added five times equably during the reaction time.

the reaction and further increasing of the amount was not that meaningful (entries 1–3). Excessive H₂O₂ and high temperature were obviously beneficial to the reaction (entries 4–6 and 8–10), but at the same time, high temperature would accelerate the decomposition of H₂O₂ and more H₂O₂ would be required to complete the reaction. So better results were achieved when H₂O₂ was added in batch (entry 7).

The effect of the reaction time on the oxidation was a little complicated. The yield was not simply growing and leveling off when prolonging the reaction time. Maximum production of 1-oxo-2,6-dichloropyrazine was obtained at 4 h, whereas after that, the yield went down, probably because of the generation of a salt between substrate 1-oxo-2,6-dichloropyrazine and CS/HWO. Because the catalyst was peroxotungstate itself, once the oxidation process completed, the product may experience a trans-salifying process. So for the oxidation of pyrazine derivatives under this system, reaction termination should be exactly controlled.

The oxidation efficiency with CS/HWO of different CS amounts was also studied. As mentioned previously, there are many free amines in CS so the amount of it could be modified. As illustrated in Figure 4, CS alone hardly showed any activity in the oxidation of 2,6-dichloropyrazine and a maximum activity was observed with 3 g CS when 4 mmol tungsten was used. With higher amount of CS, despite of the high dispersion of catalyst, the active species was not sufficient for the reaction. On the other hand, with lower amount, the aggregation of peroxotungstate lowered the dispersion, leading to a reduced conversion. Therefore, 3 g CS was used for catalyst preparation used in the following investigation.

The CH₃CN-CS/HWO system undoubtedly played an important role in exploring novel oxidation steps for synthetic of LLM-105. Based on these results, oxidation of 2,6-dichloropyrazine, 2,6-dimethoxypyrazine and 2-chloro-6-methoxypyrazine were tested respectively to explore novel synthetic pathway for LLM-105 without CF₃COOH. Good to excellent results were achieved with CS/HWO as catalyst and H₂O₂ as oxidant under the optimized reaction conditions. As can be seen from Table 3, the best reaction time for 2,6-dichloropyrazine, 2,6-dimethoxypyrazine, 2-chloro-6-methoxypyrazine and pyrazine was 4, 2, 3, and 3 h, respectively. 2,6-dimethoxypyrazine was oxidized the fastest among the pyrazine derivatives tested, probably because of the electron donating effect of –OCH₃, leading to a high cloud density on the N atom so as to be easily oxidized. And for all of the four substrates, only mono-oxidation products could be obtained.

On the basis of some previous studies [9,12], a possible mechanism for the aerobic oxidation of alcohols in the system was proposed. The catalyst is reduced by substrate to generate a reduced form (in particular the valent change of W). At the same time, substrate is oxidized to generate the product N-oxide. Finally, the catalytic cycle is completed by the reoxidation of HWO_{red} to the peroxotungstate by using H₂O₂. Simplified procedure for the catalytic degradation is generalized as shown in Scheme 3.

To further study the oxidation processes, theoretical calculations of the intermediates involved in the synthetic routes were performed.

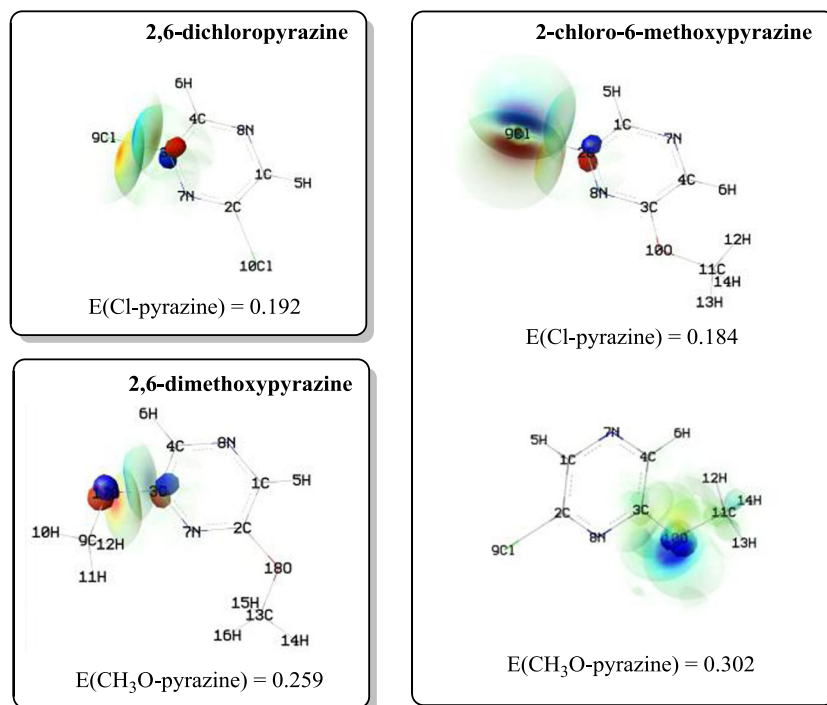
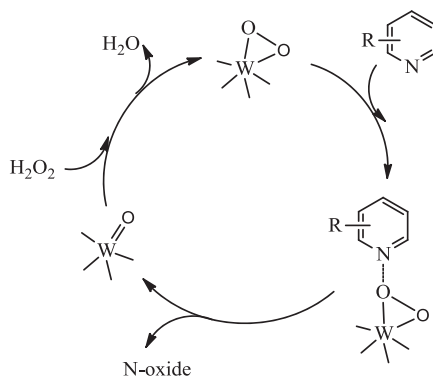


Figure 4. Second order perturbation (SOP) of 2,6-dichloropyrazine, 2,6-dimethoxypyrazine, and 2-chloro-6-methoxypyrazine. [Color figure can be viewed in the online issue, which is available at wileyonlinelibrary.com.]

Table 3
 Synthesis of oxides of pyrazine derivatives under the optimum reaction conditions^a

Entry	Substrate	Product	t(h)	Conv (%)	Yield (%)	mp (°C)
1			4	100	73	121–122
2			2	100	74	114–115
3			3	100	69	—
4			3	100	62	90–91

^aReaction conditions: substrate 10 mmol, CH₃CN 30 mL, CS/HWO 0.1 mmol (about 0.2 g), 30% H₂O₂ 5 mL was added five times equally during the reaction time, 60°C.

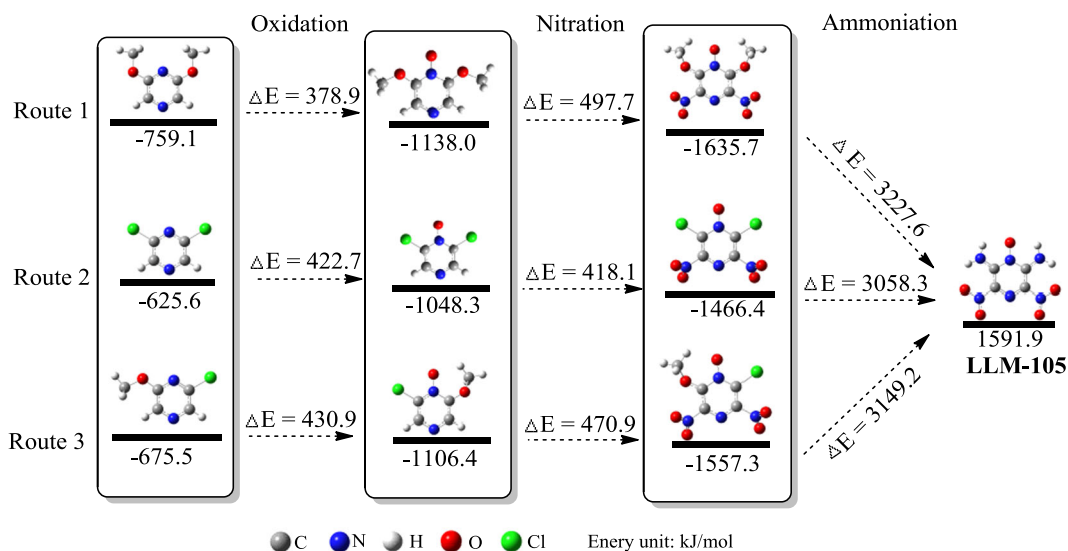
Scheme 3. The proposed mechanism for oxidation process.

The stabilities of molecules measured by zero point energy (ZPE) were calculated to evaluate the possibility of the proposed synthetic routes as shown in Figure 5. The lower the energy in value, the greater stability the molecule would obtain. As can be seen, the $-\text{OCH}_3$ group could obviously reduce the energy owing to its electron-donating property and the energy of 2,6-dimethoxypyrazine and 2-chloro-6-methoxypyrazine decreased to -675.5 and -759.1 kJ/mol, respectively. After oxidation, the energies decreased again, probably because of the coordination of peripheral electron of O to N atom, leading to the greater stability of the whole molecule. The stability of the oxidized form still followed the order of 2,6-dimethoxypyrazine > 2-chloro-6-methoxypyrazine > 2,6-dichloropyrazine. In the view of energy transformation, 2,6-dimethoxypyrazine was the easiest to be oxidized with the smallest ΔE of 378.9 kJ/mol, which was in accordance with the experimental results. The introduction of the energy group $-\text{NH}_2$ would also greatly increase the stable energy in the last step for the synthesis of LLM-105, yet its positive effect especially

intermolecular hydrogen bond was not considered in this single molecular model. The high stable energy meant that the molecule was more sensitive than the precursors. This sensitivity was the potential cause of dangerous accidents although it showed a good explosive performance.

The electron cloud density was reflected by the possibility of a single electron in a position. So the higher the data of the density, the greater the possibility of the occurrence of electrons would be. The six peripheral electrons of O atom, not full to be eight, led to an easy coordination to the N atom, as the electron on the N atom was relatively abundant compared with the whole pyrazine ring. That is to say, high electron density may be beneficial to the oxidation process. The charge distribution of 2,6-dichloropyrazine, 2,6-dimethoxypyrazine, 2-chloro-6-methoxypyrazine, and their oxidized products were listed in Figure 6, respectively. It was found that the N atom in 2,6-dimethoxypyrazine exhibited the highest electron density attributed to the electron donating property of the $-\text{CH}_3$ group, followed by 2-chloro-6-methoxypyrazine and 2,6-dichloropyrazine, respectively. After the oxidation process, the electron density on the N atom decreased greatly because of the coordination of electrons between the N and O atom. So in the view of charge distribution, 2,6-dimethoxypyrazine was still the easiest to be oxidized, which matched well with the experimental results and ZPE analysis mentioned previously.

All functional groups introduced into pyrazine could affect the property of molecule from many aspects, such as electron-withdrawing or donating and interaction to other groups [13]. The former determined the reaction difficulty in the next step including the oxidation step, whereas the later was related to the stability of the whole molecule [14]. NBO calculated with Gaussian 03 provides

**Figure 5.** The stable energy of each molecule in route 1, 2, and 3. [Color figure can be viewed in the online issue, which is available at wileyonlinelibrary.com.]

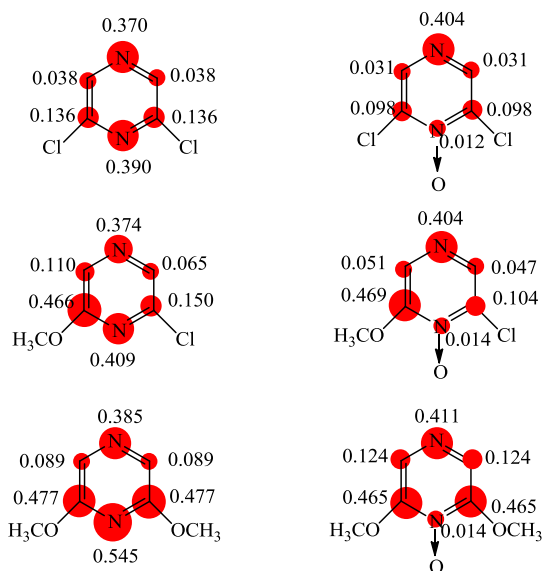


Figure 6. Charge distribution of C and N in the pyrazine ring. [Color figure can be viewed in the online issue, which is available at wileyonlinelibrary.com.]

a novel method for us to describe and explain the relative phenomenon [15]. Some important calculation results of the substrates were listed in Table 4. The interaction between donor NBO (i) and acceptor NBO (j) was described by stabilization energy E_{i-j} on the basis of the second order perturbation theory [16]. The higher the value of E_{i-j} was, the stronger their interaction would be, and thus the electrons were more likely to be shared by two orbital. Also Figure 3 gave visual statements of this interaction on the basis of the values in the tables. E showed the intensity of interaction and its change was similar with E_{i-j} .

For 2,6-dichloropyrazine, though Cl atom itself was an electron-withdrawing group, pyrazine showed a stronger electron-deficient property and thus became an acceptor.

Table 4

Natural bond orbital (NBO) of 2,6-dichloropyrazine, 2,6-dimethoxypyrazine, 2-chloro-6-methoxypyrazine.

Groups	Donor NBO (i)	Acceptor NBO (j)	E_{i-j} (kcal/mol)
2,6-dichloropyrazine			
Cl – pyrazine:	LP (3) Cl9	BD*(2) C3–C4	12.04
	LP (3) Cl10	BD*(2) C2–N7	14.14
2,6-dimethoxypyrazine			
CH ₃ O – pyrazine:	LP (2) O17	BD*(2) C3–C4	32.05
	LP (1) O18	BD*(1) C2–N7	39.45
2-chloro-6-methoxypyrazine			
Cl – pyrazine:	LP (3) Cl9	BD*(2) C2–N8	13.50
	LP (2) Cl9	BD*(1) C2–N8	5.25
CH ₃ O – pyrazine:	LP (2) O10	BD*(2) C3–C4	35.19
	LP (1) O10	BD*(1) C3–C4	7.10

Two groups of lone pair electrons in each Cl atom were shared with C–C and C–N antibonding orbital respectively. This interaction focused mainly on the C2 or C3 atom of 2,6-dichloropyrazine that could be seen obviously in Figure 6 that the electron cloud showed partiality for C atom. When –OCH₃ was introduced into pyrazine, pyrazine turned to accept the electron from –OCH₃ and another interaction center was formed at C3 of 2-chloro-6-methoxypyrazine, resulting in the weakened effect of Cl as demonstrated in Figure 3 that the electron cloud was not as tendency to C atom as that in 2,6-dichloropyrazine. The two –OCH₃ groups in 2,6-dimethoxypyrazine played the same role as in 2-chloro-6-methoxypyrazine, sharing the “exploitation” of electron by pyrazine. Thus, a decrease in $E(\text{CH}_3\text{O} - \text{pyrazine})$ was witnessed from 0.302 to 0.259. Comparing the total interaction of these functional groups, the value of E in 2,6-dimethoxypyrazine (0.259×2) with two electron-donating groups was higher than both 2,6-dichloropyrazine and 2-chloro-6-methoxypyrazine (0.192×2 , $0.184 + 0.302$), which enriched the electronic density of pyrazine so as to be beneficial for oxidation.

Based on the calculation results to compare the proposed routes, the two methoxy groups (in route 1) were beneficial to the oxidation process, and route 1 should be the most reliable one of the three. The energy transfer of oxidation process, the electron density on the N atom and the interaction between functional groups and pyrazine all indicated the possibility for the oxidation process to follow the order of 2,6-dimethoxypyrazine > 2-chloro-6-methoxypyrazine > 2,6-dichloropyrazine, showing the consistent theoretical and experimental results.

CONCLUSION

In conclusion, we have developed a new catalytic system for the oxidation reactions involved in the synthesis of LLM-105, with protonated peroxotungstate combining CS as the catalyst. Different from the traditional oxidation process in the synthetic route for LLM-105, trifluoroacetic acid was avoided completely and thus provided a significant exploration towards novel synthetic route for LLM-105. Also, all intermediates involved in oxidation process and synthesis of LLM-105 were evaluated by Gaussian 03 NBO, charge distribution, and ZPE were discussed to describe the complexity of the oxidation process for 2,6-dichloropyrazine, 2-chloro-6-methoxypyrazine, 2,6-dimethoxypyrazine respectively. All of the theoretical data matched well with experimental results. And synthesis of other N-oxides under CS/HWO system is still ongoing.

EXPERIMENTAL SECTION

Materials and methods. All the solvents and reagents employed in the work were used as received from Sinopharm

Chemical Reagent Co., Ltd (China) unless otherwise stated. NMR spectra were recorded on Bruker DRX500 spectrometer (Bruker, Zürich, Switzerland). IR spectra were recorded on NICOLET NEXUS870 (Nicolet Company, USA). TGA was performed on TGA/SDTA851e (Mettler Toledo, Switzerland) under air atmosphere from 50 to 800°C, with a heating rate of 20°C/min, and an air flowing rate of 30 mL/min.

Preparation of the catalyst. A suspension of H₂WO₄ (1 g, 4 mmol) in 30% aqueous H₂O₂ (4 mL, 40 mmol) was stirred at 32°C for 90 min until a pale yellow solution was obtained. Chitosan (CS, deacetylated degree 85~95 wt.%, viscosity 50~800 mPa s, 3 g) dissolved in 40 mL H₂O was added into the solution. The resulting solution was stirred for another 30 min before filtration to get yellow precipitate of CS immobilized peroxotungstate CS/WO. For the protonation process, CS/WO (1.5 g, about 1.2 mmol for tungsten), and 70% HNO₃ (0.18 g, 2 mmol) were dissolved in a solution of 30% aqueous H₂O₂ (1 mL) in DMSO (10 mL). After it was stirred for 30 min, excessive water was added to the mixture with white crystals generated. Then the white solid of protonated peroxotungstate CS/HWO was obtained through filtration

Synthesis of 2,6-dimethoxypyrazine. 2,6-dichloropyrazine (1.49 g, 10 mmol) was added to into a fresh sodium methylate-methanol solution (25% wt.%, 1.16 g Na, 12.2 mL methanol) at 0°C, and the reaction mixture was heated at reflux for 3 h. After cooling down, the mixture was poured into 100 mL ice-water mixture and filtrated. The filtrate was extracted with CH₂Cl₂ (3 × 20 mL) and combined with the filter cake dissolved in dichloromethane, followed by drying over anhydrous magnesium sulfate. The colorless solid was obtained by vacuum distillation with a yield of 1.36 g (97%), mp 29–30°C. ¹H-NMR (500M, CDCl₃) δ ppm: 3.88 (s, 6H), 7.71 (s, 2H); ¹³C-NMR (125 M, CDCl₃) δ ppm: 52.96, 123.98, 158.46.

Synthesis of 2-chloro-6-methoxypyrazine. 2-Chloro-6-methoxypyrazine was synthesized according to reference [17]. 2,6-Dichloropyrazine (1.49 g, 10 mmol) was added to a solution of sodium methylate NaOCH₃ (0.2 M solution in CH₃OH, 50 mL, 10 mmol) at 0°C, and the reaction mixture was heated at reflux for 14 h. After cooling to room temperature, the mixture was concentrated with rotary evaporation *in vacuo*. The residue was partitioned between saturated NaCl solution (20 mL) and CH₂Cl₂ (20 mL), then the aqueous phase was further extracted with CH₂Cl₂ (2 × 20 mL) and the combined organic washings were dried over MgSO₄, filtered, and concentrated *in vacuo*. Purification by column chromatography [n-hexane: EtOAc (9:1)] yielded 2-chloro-6-methoxypyrazine (0.95 g, 66%) as a colorless oil. ¹H-NMR (500 M, CDCl₃) δ ppm: 3.99 (s, 3H), 8.13 (s, 1H), 8.15 (s, 1H); ¹³C-NMR (125 M, CDCl₃) δ ppm: 53.87, 132.70, 134.68, 145.03, 159.20.

Synthesis of oxidized pyrazine derivatives. Substrate (10 mmol), CH₃CN (30 mL), were introduced into a 100-mL three-neck flask. 30% H₂O₂ (5 mL) was added five times equably during the reaction time. The reaction was initiated by addition of the catalyst CS/HWO (0.1 mmol, about 0.2 g), and allowed to go on at 60°C temperature for a certain time. The oxidation process was monitored by TLC. After the termination of oxidation, the mixture was filtered to remove the catalyst and concentrated *in vacuo*. Only with vacuum drying, the catalyst could be reused without further treatment.

The residue was then extracted with CH₂Cl₂ for three times and the combined organic washings were dried over MgSO₄, filtered, and concentrated *in vacuo*. Further purification was carried out by using column chromatography. For 1-oxo-2,6-dichloropyrazine petroleum ether (PE): EtOAc=8:2; ¹H-NMR (500 M, CDCl₃) δ ppm: 1.59 (s, 1H), 8.08 (s, 1H); ¹³C-NMR (125 M, CDCl₃) δ ppm: 131.94, 149.49. For 1-oxo-2,6-dimethoxypyrazine, PE: EtOAc=8:2; ¹H-NMR (500 M, CDCl₃) δ ppm: 3.98 (s, 6H), 7.47 (s, 2H); ¹³C-NMR (125 M, CDCl₃) δ ppm: 53.90, 115.32, 161.18. For 1-oxo 2-chloro-6-methoxypyrazine, PE: EtOAc=5:5; ¹H-NMR (500 M, CDCl₃) δ ppm: 4.01 (s, 6H), 7.6997–7.7019 (m, 1H), 7.8095–7.8116 (m, 1H); ¹³C-NMR (125 M, CDCl₃) δ ppm: 54.72, 121.07, 126.93, 147.26, 162.00. For 1-oxo-pyrazine, methanol: EtOAc=5:95; ¹H-NMR (500 M, CDCl₃) δ ppm: 8.1162–8.1261 (m, 2H), 8.4801–8.4895 (m, 2H); ¹³C-NMR (125 M, CDCl₃) δ ppm: 133.71, 136.06, 147.23, 147.47.

Computational details. B3LYP/6-31G++(d,p) were carried out using Gaussian 03.²⁶ Global minima of structures for use were first computed and listed in the Supporting Information. ZPE with enthalpy corrections and NBO based on these structures were used to determine the energy surface and interaction between the functional groups of each molecule.

Acknowledgments. We thank the NSAF and NSFC of China (no. 11076017) and the Scientific Innovation Program of Jiangsu Province (no. CXZZ11_0264) for support of this research.

REFERENCES AND NOTES

- [1] (a) Korkin, A. A.; Bartlett, R. J. *J Am Chem Soc* 1996, 118, 12244; (b) Fried, L. E.; Manaa, M. R.; Pagoria, P. F.; Simpson, R. L. *Annu Rev Mater Res* 2001, 31, 291; (c) Strout, D. L. *J Phys Chem A* 2004, 108, 10911.
- [2] (a) Lee, R. S.; Cutting, J. L.; Hodgins, R. L.; Pagoria, P. F.; Simpson, R. L.; Souers, P. C. The 11th International Detonation Symposium, 1998, UCRL-JL-127795; (b) Cutting, J. L.; Hodgins, R. L.; Hoffman, M. D.; Garcia, F.; Lee, R. S.; McGuire, E.; Mitchell, A. R.; Pagoria, P. F.; Schmidt, R. D.; Simpson, R. L.; Souers, P. C. The 11th International Detonation Symposium, 1998, UCRL-JL-131623; (c) Tarver, C. M.; Urtiew, P. A.; Tran, T. D. *J Energ Mater* 2005, 23(3), 183.
- [3] (a) Pagoria, P. F. JOWOG 9 meeting, 1997, UCRL-JC-117228; (b) Pagoria, P. F. JOWOG 9 meeting, 1998, UCRL-JC-130518.
- [4] (a) Pagoria, P. F.; Mitchell, A. R.; Schmidt, R. D. Munitions Technology Development Program, 1999, UCRL-ID-103483-99; (b) Pagoria, P. F.; Lee, G. S.; Mitchell, A. R.; Schmidt, R. D. The Synthesis of Amino- and Nitro-Substituted Heterocycles as Insensitive Energetic Materials. UCRL-JC-142918, 2001.
- [5] (a) Tran, T. D.; Pagoria, P. F.; Hoffman, M. D.; Cunningham, B.; Simpson, R. L.; Lee, R. S.; Cutting, J. L. The 12th International Detonation Symposium, 2002, UCRL-JC-144963; (b) Li, H. B.; Cheng B. B.; Li H. Z. *Chin. J Org Chem* 2007, 27, 112 (in Chinese).
- [6] Deng, Z. M.; Ye, Z. H.; Su, H. P. *Chin. J Explos & Propell* 2009, 32(4), 50 (in Chinese).
- [7] Pagoria, P. F. US patent 20090299067A1, 2009
- [8] (a) Bregeault, J. M.; Vennat, M.; Salles, L.; Piquemal, J. Y.; Mahha, Y.; Briot, E.; Bakala, P. C.; Atlamsani, A.; Thouvenot, R. *J Mol Catal A*, 2006, 250, 177; (b) Kamata, K.; Ishimoto, R.; Hirano, T.; Kuzuya, S.; Uehara, K.; Mizuno, N. *Inorg Chem* 2010, 49, 2471.
- [9] Ishimoto, R.; Kamata K.; Mizuno, N. *Angew Chem Int Ed* 2012, 51, 4662.
- [10] El Kadib, A.; Bousmina, M. *Chem Eur J* 2012, 18, 8264.
- [11] Cui, Z. M.; Xing, W.; Liu, C. P.; Liao, J. H.; Zhang, H. J. *Power Sources* 2009, 188, 24.

- [12] (a) Kamata, K.; Hirano, T.; Kuzuya, S.; Mizuno, N. *J Am Chem Soc* 2009, 131, 6997; (b) Kamata, K.; Yamaguchi, K.; Hikichi, S.; Mizuno, N. *Adv Synth Catal* 2003, 345, 1193.
- [13] Alabugin, I. V.; Manoharan, M. S.; Peabody, S.; Weinhold, F. *J Am Chem Soc* 2003, 125, 5973.
- [14] (a) Cossi, M.; Scalmani, G.; Rega, N.; Barone, V. *J Chem Phys* 2002, 117, 43; (b) Mahesvari, S.; Chowdury, A.; Sathyamurthy, N.; Mishra, H.; Tripathi, H. B.; Panda, M.; Chandrasekhar, J. *J Phys Chem A* 1999, 103, 6257; (c) Liu, X.; Zhou, X.; Shu, X.; Zhu, J. *Macromolecules* 2009, 42, 7634.
- [15] Frisch, M. J., et al. *Gaussian 03*, Revision C.02; Gaussian, Inc.: Wallingford CT, 2004.
- [16] Cheng, C.; Shyu, S. F.; Hsu, F. S. *J Quantum Chem* 1999, 74, 395.
- [17] Hirschhäuser, C.; Haseler, C. A.; Gallagher, T. *Angew Chem Int Ed* 2011, 50, 5162.